

The Effects of the Misfit Structure on Thermoelectric Properties of $\text{Bi}_{2-x}\text{Pb}_x\text{Sr}_2\text{Co}_2\text{O}_y$ Single Crystals

T. Fujii and I. Terasaki

Department of Applied Physics, Waseda University, Tokyo 169-8555, Japan
 Precursory Research for Embryonic Science and Technology,
 Japan Science and Technology Corporation, Kawaguchi 332-0012, Japan
 fujii@htsc.sci.waseda.ac.jp

Abstract

In-plane anisotropy of the resistivity and thermopower was measured for single crystal $\text{Bi}_{2-x}\text{Pb}_x\text{Sr}_2\text{Co}_2\text{O}_y$. There is large in-plane anisotropy, which is attributed to the anisotropic pseudogap formation due to the different crystal symmetry between the square $\text{Bi}_2\text{Sr}_2\text{O}_4$ layer and the triangular CuO_2 layer. The magnitude of the thermopower both along a - and b -axis direction increases with Pb doping from $x=0$ to 0.4, where we observe discontinuous shrink of b -axis length. We attribute this to the enhancement of the misfitness. Thus, we can improve the thermoelectric properties by tuning the misfitness.

Introduction

Since NaCo_2O_4 was found to show large thermopower (100 $\mu\text{V}/\text{K}$ at 300 K) and low resistivity (200 $\mu\Omega\text{cm}$ at 300 K) [1], the layered Co oxides are expected to be a candidate for thermoelectric materials [2-5]. They are characterized by a two-dimensional CoO_2 layer, which consists of edge-shared CoO_6 octahedra responsible for the electric conduction and the large thermopower. Among them, $\text{Bi}_2\text{Sr}_2\text{Co}_2\text{O}_y$ was first thought to have a structure isomorphic to that of the high- T_c Cu oxide $\text{Bi}_2\text{Sr}_2\text{CaCu}_2\text{O}_{8+\delta}$ (Bi-2212) because these two compounds have almost same lattice constants. However, it turned out to be a “misfit compound”, where the rock-salt type square $\text{Bi}_2\text{Sr}_2\text{O}_4$ layer lies on the CdI_2 -type triangular CoO_2 layer with lattice misfit along the b axis [6]. Another striking feature of the crystal structure in the Bi based layered oxides, is modulation structure [7], which disappears by the substitution of Bi by Pb [8].

From the viewpoint of the group theory, the hexagonal CoO_2 layer in $\text{Bi}_2\text{Sr}_2\text{Co}_2\text{O}_y$ and the square CuO_2 layer in Bi-2212 themselves should have no in-plane anisotropy in the thermopower and resistivity. However, in some cases, in-plane anisotropy in the resistivity can be observed [9]. A possible origin of the in-plane anisotropy is the self-organization of the electronic system into quasi-one-dimensional stripes. The enhancement of the in-plane anisotropy of the resistivity ρ_a/ρ_b has been reported in the lightly doped high- T_c Cu oxide $\text{La}_{2-x}\text{Sr}_x\text{CuO}_4$ and $\text{YBa}_2\text{Cu}_3\text{O}_y$, and has been associated with the charge-stripes [10].

In the case of the $\text{Bi}_2\text{Sr}_2\text{Co}_2\text{O}_y$, the coupling between the square $\text{Bi}_2\text{Sr}_2\text{O}_4$ layer and the triangular CoO_2 layer is considered to be strong. Then, the stack of different symmetry layers would induce the in-plane anisotropy in the physical properties. Moreover, the lattice misfit between these two layers is thought to induce chemical pressure along the b -axis

direction. It is, then, interesting how the electric properties are affected by these misfit structures. Here, we have grown the large single crystal of $\text{Bi}_{2-x}\text{Pb}_x\text{Sr}_2\text{Co}_2\text{O}_y$ by using traveling solvent floating zone (TSFZ) method, and have measured the in-plane anisotropy on the resistivity and thermopower.

Experimental

Single crystals of $\text{Bi}_{2-x}\text{Pb}_x\text{Sr}_2\text{Co}_2\text{O}_y$ ($x=0, 0.4, \text{ and } 0.6$) were grown by TSFZ method at a growth rate of 0.5 mm/h in a mixed gas flow of O_2 (20%) and Ar (80%). The starting compositions for all Pb concentrations were applied (Bi,Pb) : Sr : Co = 2 : 2 : 2. Large single crystals with dimensions up to $5*4*0.5 \text{ mm}^3$ were successfully grown.

The grown crystals were characterized by a four-circle x-ray diffractometer (Cu K_α x-ray source) and a transmission electron microscope (TEM). The actual composition was analyzed through inductively coupled plasma-atomic emission spectroscopy (ICP) and energy dispersive x-ray analysis (EDX). a - and b -axis resistivities were measured by a standard four-probe method using different samples cleaved along a - and b -axis directions. a - and b -axis thermopowers were measured by a steady-state technique using the same sample changing the measurement configurations.

Results and Discussion

Samples used for this study are listed in Table 1 with the actual chemical compositions. Hereafter, we refer to these samples as nominal Pb concentration. The actual compositions of Pb measured by ICP and EDX correspond well with the nominal compositions. We analyze several samples for each Pb concentration, and confirm the homogeneity of the samples.

Since $\text{Bi}_{2-x}\text{Pb}_x\text{Sr}_2\text{Co}_2\text{O}_y$ has very complicated structure as explained above, it was difficult to perform single-crystal structure analysis. We manually searched the diffraction peak using the reported lattice constants. The obtained lattice

Table 1. Chemical composition estimated from energy dispersive x-ray (EDX) analysis and inductively coupled plasma-atomic emission spectroscopy (ICP).

		Bi	Pb	Sr	Co
x=0	EDX	2.21	0	2.20	2.0
	ICP	2.10	0	2.10	2.0
x=0.4		1.61	0.40	2.09	2.0
		1.82	0.42	2.18	2.0
x=0.6		1.58	0.57	2.13	2.0
		1.60	0.60	2.10	2.0

parameters are shown in Fig. 1 plotted against actual composition. The data from the previous report are also shown [11], where the lattice constants were estimated from a powder XRD measurement using crushed single crystals. These results well correspond to each other. Since Co atoms have large mass absorption coefficient for Cu K_α radiation, observed reflections come from the rock-salt $\text{Bi}_2\text{Sr}_2\text{O}_4$ layer. Thus, we refer a - and b -axis lengths obtained here as a_{RS} - and b_{RS} -axis. The c -axis length monotonically increases with increasing Pb concentration due to the large ion radius of Pb. Note that the b_{RS} -axis length discontinuously shrink with Pb concentration from $x=0$ to 0.4. While, the a_{RS} -axis length does not change with Pb concentration.

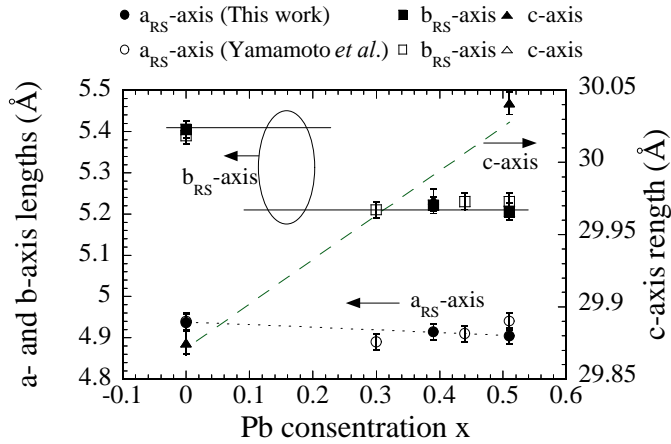


Figure 1. The lattice parameter characterized by a four-circle x-ray diffractometer. Previous data estimated from powder x-ray diffractometer using crushed single crystals is also shown.

Figures 2(a) and (b) show the TEM diffraction patterns of $\text{Bi}_{2-x}\text{Pb}_x\text{Sr}_2\text{Co}_2\text{O}_y$ [(a): $x=0$ and (b): 0.4]. The hexagonal diffraction patterns from the CoO_2 layer and the square diffraction patterns from the $\text{Bi}_2\text{Sr}_2\text{O}_4$ layer are clearly observed. The b -axis length of the hexagonal CoO_2 layer b_H is independent of Pb concentration within the resolution limit, and is about 2.8 Å. From these two diffraction pattern images, we notice that the distance between the (020_H) and (040_{RS}) spot of $x=0$ is narrower than that of $x=0.4$, indicating the enhancement of misfit. Another remarkable difference between TEM diffraction patterns is the satellite diffraction patterns along the oblique direction from a_{RS}^* and b_{RS}^* seen in the $x=0$ sample. This satellite diffraction patterns are due to the modulation structure, which is also observed in high- T_c Cu oxide $\text{Bi}_2\text{Sr}_2\text{CaCu}_2\text{O}_{8+\delta}$. The modulation structure was confirmed by the Laue transmission photographs with incident x-ray beam perpendicular to the ab -plane. Figure 2(c) and (d) show the Laue patterns of $x=0$ and 0.4 samples respectively. A two-fold symmetry Laue pattern, where an axis of symmetry is tilted about 45° from a_{RS}^* or b_{RS}^* axis, can be observed, while the Laue pattern of $x=0.4$ sample shows a four-fold symmetry along the a_{RS}^* and b_{RS}^* axes. This two-fold symmetry Laue pattern agrees well with that of superconducting compound Bi-2212, which have modulation structure [12].

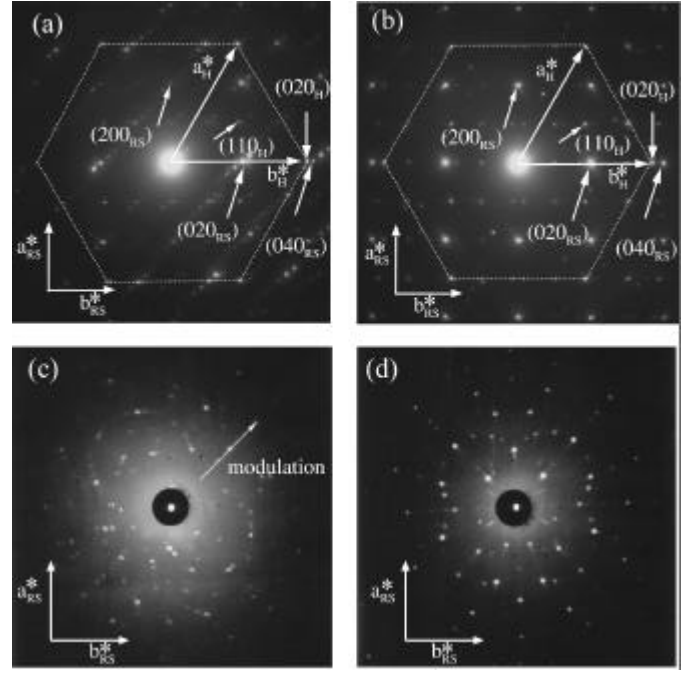
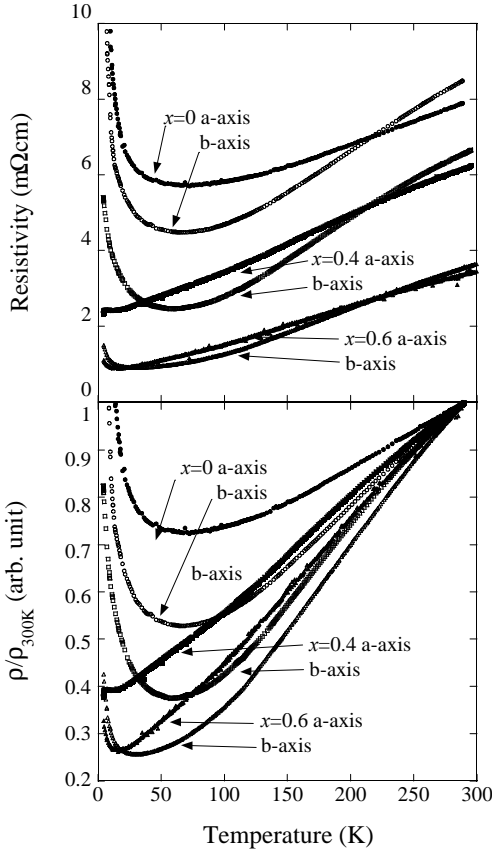


Figure 2. TEM diffraction patterns of $\text{Bi}_{2-x}\text{Pb}_x\text{Sr}_2\text{Co}_2\text{O}_y$ [(a): $x=0$ and (b): 0.4]. Laue transmission photographs with incident x-ray beam perpendicular to the ab -plane [(c): $x=0$ and (d): 0.4]

Figure 3(a) shows the temperature dependence of the a - and b -axis (of the rock-salt layer) resistivities for various Pb concentrations. The magnitude of the resistivity decreases with increasing Pb concentration, indicating carrier doping by the substitution of divalent Pb for trivalent Bi. These resistivities are normalized at room temperature in Fig. 3(b). The slope of the resistivity increases with Pb concentration, which also indicates the carrier doping. In a rough estimation of the carriers based on the nominal composition, 20% ($x=0.4$) substitution of Pb introduces 0.2 hole per Co atoms. The decrease of the resistivity from $x=0$ to 0.4 at room temperature seems to be smaller than expected from the above estimation. Actually, reported Hall coefficient does not change very much, which indicate that less than 0.05 hole per Co atoms is introduced by 20% substitution of Pb [13]. On the other hand, Pb substitution strongly suppresses the upturn behavior at low temperatures. These results suggest that the Pb substitution works not only as carrier doping, but also changes the electronic structure of the CoO_2 layer.

Figures 4(a)-(c) show the temperature dependence of the thermopower measured along the a - and b -axis directions. The magnitude of the thermopower of both directions increases with increasing Pb concentration from $x=0$ to 0.4. In conventional thermoelectric materials, the thermopower and the resistivity depend on the carrier concentration, and the thermopower is expected to decrease when the resistivity decreases with increasing carrier concentration. Thus the increase in the thermopower is considered to be due to the discontinuous shrink of the rock-salt b -axis length, which overcomes the decrease of the thermopower by doping. The chemical pressure induced by the misfit structure enhances the



Figurers 3. (a) Temperature dependence of the a - and b -axis resistivities. (b) They are normalized at room temperature.

thermopower as is seen in the pressure dependence of the thermopower in the Ce-based compound [14].

On the other hand, the thermopower decreases with further Pb doping from $x=0.4$ to 0.6 . Since the crystal structure is nearly unchanged, observed decrease in the thermopower and resistivity is attributed to the increase of the carrier concentration.

Next we will discuss the in-plane anisotropy in the resistivity (ρ_b/ρ_a) and thermopower (S_b/S_a). Figures 5(a) and (b) show the temperature dependence of ρ_b/ρ_a and S_b/S_a , respectively. For all Pb concentrations, ρ_b/ρ_a decreases with decreasing temperature near the room temperature, while it increase rapidly below 80 K, which indicate that ρ_a is more conductive than ρ_b in low temperature. ρ_b/ρ_a of $x=0.4$ is as large as 2.5 at 4.5 K, while ρ_b/ρ_a of $x=0.6$ decreases due to the suppression of the upturn along the b -axis. We have previously proposed that the large in-plane anisotropy is come from the anisotropic pseudogap formation. If the misfit structure lowers the crystal symmetry of the CoO_2 layer to induce the spin-density-wave-like state, the anisotropic pseudogap would be open [9]. Actually, S_b/S_a and ρ_b/ρ_a are considered to be dominated by the density of states, because the magnitude and the temperature dependence of S_b/S_a and ρ_b/ρ_a roughly correspond to each other.

On the other hand, the increase in the anisotropy at low temperature is quantitatively very similar to lightly doped high- T_c Cu oxides $\text{La}_{2-x}\text{Sr}_x\text{CuO}_4$ ($x=0.02-0.04$) and $\text{YBa}_2\text{Cu}_3\text{O}_y$ ($y=6.35-6.55$). These large in-plane anisotropies

in high- T_c Cu oxide have been discussed in relation to the stripe order [10]. Since the triangular CoO_2 layer itself no in-plane anisotropy, large in-plane anisotropy in the resistivity suggests the self-organization of the electronic system as high- T_c Cu oxide.

By looking carefully, one can find that ρ_b/ρ_a of $x=0$ is somewhat smaller than S_b/S_a . We attribute this to the modulation structure, which works as an anisotropic scattering center in Bi-2212 [15]. The anisotropy would be averaged by the modulation structure, whose direction is tilted by 45 degrees from the a - and b -axis direction.

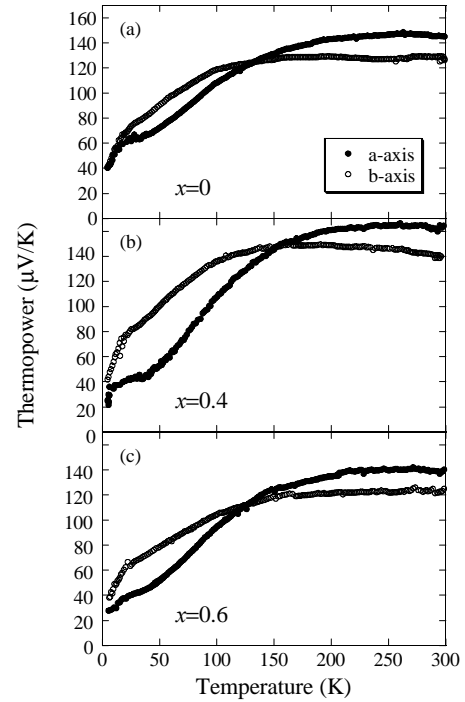


Figure 4. Temperature dependence of the thermopower along a - and b -axes.

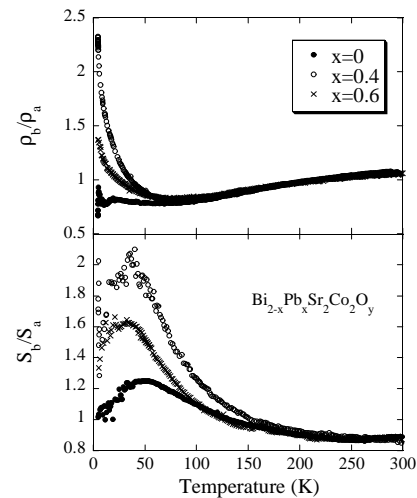


Figure 5. In plane anisotropy in the resistivity (ρ_b/ρ_a) and thermopower (S_b/S_a).

Conclusions

We have successfully grown the large single crystal of $\text{Bi}_{2-x}\text{Pb}_x\text{Sr}_2\text{Co}_2\text{O}_y$ by TSFZ method and measured the in-plane anisotropy in the resistivity and thermopower. From the structural analysis, significant change in the b_{RS} -axis length of the rock salt $\text{Bi}_2\text{Sr}_2\text{O}_4$ layer has observed between $x=0$ and 0.4, which causes the enhancement of the misfit. The 15% increase in thermopower is due to the increase of the chemical pressure, as seen in the Ce-based compounds. These results indicate the thermoelectric properties can be controlled by controlling the misfit. There is a large in-plane anisotropy in the resistivity and thermopower. The anisotropic pseudogap formation at low temperatures would make the resistivity nonmetallic and the thermopower larger along the b -axis direction. Another scenario of the large in-plane anisotropy is a charge stripe as seen in the lightly doped high- T_c superconductor. In the case of the resistivity for $x=0$, the modulation structure along the oblique direction from the a_{RS} - and b_{RS} -axis averages the anisotropy.

Acknowledgments

I would like to thank A. Matsuda and T. Watanabe for collaboration at the early stage of this work and also appreciate T. Goto and S. Enomoto for crystal characterization.

References

1. I. Terasaki, Y. Sasago, and K. Uchinokura, "Large thermoelectric power of NaCo_2O_4 single crystals", *Phys. Rev. B*, Vol. 56, No. 20, pp. R12685-R12687 (1997).
2. R. Funahashi and I. Matsubara, "Thermoelectric properties of Pb-free and Ca-based $(\text{Bi}_2\text{Sr}_2\text{Co}_4)_x\text{CoO}_2$ whiskers" *Appl. Phys. Lett.*, Vol. 79, No. 3, pp. 362-364 (2001).
3. T. Ito and I. Terasaki, "Thermoelectric Properties of $\text{Bi}_{2.3-x}\text{Pb}_x\text{Sr}_{2.6}\text{Co}_2\text{O}_y$ Single Crystals", *Jpn. J. Appl. Phys.*, Vol. 39, No. 12A, pp. 6658-6660 (2000).
4. S. Li, R. Funahashi, I. Matsubara, K. Ueno, and H. Yamada, "High temperature thermoelectric properties of oxide $\text{Ca}_9\text{Co}_{12}\text{O}_{28}$ ", *J. Mater. Chem.*, Vol. 9, pp. 1659-1660 (1999).
5. Y. Miyazaki, K. Kudo, M. Akoshima, Y. Ono, Y. Koike, and T. Kajitani, "Low-Temperature Thermoelectric Properties of the Composite Crystal $[\text{Ca}_2\text{CoO}_{3.34}]_{0.614}[\text{CoO}_2]$ ", *Jpn. J. Appl. Phys.*, Vol. 39, No. 6A, pp. L531-L533 (2000).
6. H. Leligny, D. Grebille, O. Perez, A. -C. Masset, M. Hervieu, C. Michel, and B. Raveau, "A bismuth cobaltite with an intrinsically modulated misfit layer structure: $[\text{Bi}_{0.87}\text{SrO}_2]_2[\text{CoO}_2]_{1.82}$ ", *C. R. Acad. Sci. Paris, Serie 2c*, Vol. 2, pp. 409-414 (1999).
7. Y. Matsui, A. Maeda, Y. Tanaka, and S. Horiuchi, "Possible Model of the Modulated Structure in High- T_c Superconductor in a Bi-Sr-Ca-Cu-O System Revealed by High-Resolution Electron Microscopy", *Jpn. J. Appl. Phys.*, Vol. 27, L372-L375 (1988).
8. Y. Matsui, A. Maeda, K. Uchinokura and S. Takekawa, "Transmission Electron Microscopy of Modulated Structures in Pb-doped BSCO Superconductors, $\text{Bi}_{2.1-x}\text{Pb}_x\text{Sr}_{1.9}\text{CuO}_y$ ($x=0$ to 0.3)", *Jpn. J. Appl. Phys.*, Vol. 29, No. 2, pp. L273-L276 (1990).
9. T. Fujii, I. Terasaki, T. Watanabe, and A. Matsuda, "Large In-Plane Anisotropy on Resistivity and Thermopower in the Misfit Layered Oxide $\text{Bi}_{2-x}\text{Pb}_x\text{Sr}_2\text{Co}_2\text{O}_y$ ", *Jpn. J. Appl. Phys.*, Vol. 41, No. 7A, pp. L783-786 (2002).
10. Y. Ando, K. Segawa, S. Komiya, and A. N. Lavrov, "Electrical Resistivity Anisotropy from Self-Organized One Dimensionality in High-Temperature Superconductors", *Phys. Rev. Lett.*, Vol. 88, No. 13, pp. 137005 (2002).
11. T. Yamamoto, I. Tsukada, K. Uchinokura, M. Takagi, T. Tsubone, M. Ichihara and K. Kobayashi, "Structural phase Transition and Metallic Behavior in Misfit Layered (Bi,Pb)-Sr-Co-O System", *Jpn. J. Appl. Phys.*, Vol 39, No. 7B, pp. L747-750 (2000).
12. J. H. P. M. Emmen, S. K. J. Lenczowski, J. H. J. Dalderop and V. A. M. Brabers, "Crystal growth and annealing experiments of the high T_c superconductor $\text{Bi}_2\text{Sr}_2\text{CaCu}_2\text{O}_{8+\delta}$ ", *J. Crystal Growth*, Vol. 118, pp. 477-482 (1992).
13. T. Yamamoto and K. Uchinokura, "Physical properties of the misfit-layered (Bi,Pb)-Sr-Co-O system: Effect of hole doping into a triangular lattice formed by low-spin Co ions", *Phys. Rev. B*, Vol. 65, pp. 184434-1-12 (2002).
14. P. Link, D. Jaccard and P. Lejay, "The thermoelectric power of CePd_2Si_2 and CeCu_2Ge_2 at very high pressure", *Physica B*, Vol. 255, pp. 207-213 (1996).
15. T. Fujii, I. Terasaki, T. Watanabe and A. Matsuda, "In-plane anisotropy on the transport properties in the modulated Bi_2O_2 -based conductors Bi_{2212} and Bi-Sr-Co-O ", to be published in *Physica C*, cond-mat/0204187.